Al-Noor Journal of Engineering Management and Computer Science

ISSN: 3079-0689 (Online)

https://njemcs.edu.iq/index.php/njemcs/

Investigational Survey of Heat Transfer in Heat Exchanger Containing Al2O3 as Nano-Fluid

Nisreen Mezher Rahmah[1], Abdulhassan A. Karamallah[2], Laith Jaafer Habeeb[3]

[1]University of Almustansiriya, Mechanical Engineering Department, Baghdad, Iraq.
[2]University of Technology, Mechanical Engineering Department, Baghdad, Iraq.
[3]University of Technology, Training and Workshops Center, Baghdad, Iraq.

ARTICLE INFO

Article history:
Received 03 November 2024,
Revised 03 November 2024,
Accepted 07 November 2024,
Online 08 November 2024

Keywords:
Heat transfer
Nano-Fluid
Heat Exchanger

ABSTRACT

In this work, the flow and the improvement of transference of heat features of distilled water and metal oxide of Al_2O_3 as Nanofluid are studied. The concentrations of nanoparticles in distilled water are 0.1, 1, 3, % by volume in a dual-pipe heat exchanger have been considered. It is composed of concentric tubes with a length of 82 cm. External tube from PVC with length (50.8 mm) and internal tube from Copper with length (12.7 mm). The cooling fluid flows in the annulus at atmospheric temperatures are (23-33) °C whereas the hot fluid flows in the internal tube at temperatures are (40, 50, 60 and 70) °C. The outcomes exhibit that the temperature rises as moving from the water to Nanofluid, whereas the average temperature alongside the inner pipe in common stay constant with the rise in the rate of flow. Likewise, the alteration in fluid characteristic raises the Nusselt number values. The Nanofluid has a Nusselt number higher than the water. The Nusselt number of Nanofluid rise with rising concentration (0.1, 1 and 3 %), as the concentration rises, the Nusselt number rises to (25.5) at (flow rate 1.5 L/min, T=70 ^oC, and ϕ=3 %). The pressure drop rise (164.8 pa) with rising concentration. Friction factor drops (0.04) at ϕ=3 % as Reynolds number rises.

1. Introduction

The nanoparticles used in nanofluids contain chemically stable metals, oxides of metal, carbides of metal, nitrides of metal, and several forms of carbon and functionalized nanoparticles. Thermal conductivities of solids higher than conventional heat transfer fluids. So those nanoparticles are suspended in fluids to advance the performance of heat transfer of the conventional heat transfer fluids.

Such particles settle down quickly, clog flow channels, erode pipelines and cause severe pressure drops [1]. From the current studies on heat transfer of Nanofluids, the thermal conductivities were more than the other

Corresponding author E-mail address: Laith.J.Habeeb@uotechnology.edu.iq

conventional fluids thermal conductivity, have a powerfully non-linear temperature dependence on the operative thermal conductivity, improve or decrease transfer of heat in one-phase flow, nanofluids result in improve mentor reduction pool nucleate boiling heat transfer, and they harvest critical higher heat fluxes when establishing boiling pool conditions. The double-pipe heat exchangers are one of the humblest kinds of heat exchangers. Ben et al. [2] studied experimentally the free and forced convection of nanofluid (Al_2O_3 water) within an inclined copper pipe subjected to a wall unvarying heat flux at its outer direction. The effect of several concentrations of nanoscale particles as well as the power supply on the improvement of the thermal field was discovered for laminar flow condition. A small lessening in the heat transfer coefficient was noted when the particle volume concentration rises from 0 to 4%. Chandrasekar and Senthilkumar [3] studied experimentally the entirely developed laminar and turbulent flow convective heat transfer features in a horizontal tube heated uniformly with Al_2O_3/water nanofluid flowing inside. With and without an inserted wire coil. For this aim, 43 nm size Al_2O_3 nanoparticles were characterized, synthesized, and sprinkled in distilled water to formulate Al_2O_3/water nanofluid consist of nanoparticles volume concentration of 0.1, 0.15 and 0.2%. The outcomes afford investigational proof that the thermophoresis mechanism shows a vital role in clarifying the improvement of heat transfer perceived with nanofluids. Heyhat et al. [4] examined the convective heat transfer and friction feature of nanofluids in a circular tube experimentally. The examination fluid was prepared using Al_2O_3 nanoparticles with 40 nm in diameter, which was sprinkled in distilled water with different volume concentrations of (0.1–2) %. Upper coefficient of heat transfer was proved for Nanofluids when related to the base fluid. If the concentrations of the particles rise, the convective heat transfer coefficient rises. Furthermore, a slight effect of Reynolds number on improvement in the transference of heat was proved. Demir et al. [5] examined the forced convection flows of Nano fluids in a horizontal tube with constant wall temperature mathematically. The Nanofluids were prepared from Al_2O_3 and TiO_2 nanoparticles that sprinkled in water. A CFD program was utilized to make the model of the horizontal test section. Mathematical outcomes exhibited that the transfer of heat improvement because of the existence of the nanoparticles in the fluid in harmony with the outcomes of the investigational study used for the numerical model validation process. Akbari et al. [6] examined the CFD foretelling of laminar mixed convection of Al2O3 water Nano fluids mathematically by single-phase, and three various two-phase models are compared. It was found that models of single-phase and two-phase predict almost equal hydrodynamic fields but very different thermal ones. The outcomes are calculated for two Reynolds numbers (1050 and 1600) and three nanoparticle volume concentrations (<2%). Mostafa et al. [7] examined the effect of convective heat transfer on the flow of nanofluid mathematically by using computational fluid dynamics in the emerging are of a pipe with continuous heat flux. In their research, nanofluid was be made of Al_2O_3 and water as a liquid single phase. Two average particle sizes (45 and 150 nm) were utilized with four concentrations of (1, 2, 4 and 6) wt. %) of particles. A very good agreement was getting between the expected data with trial data from the literature. Only 10 % was stated as the maximum error.

In this work, our contribution was heat transfer enhancement using 50 % distilled water added to 50 % Ethylene glycol, 100 % Ethylene glycol (EG), and nanofluid type Al_2O_3 metal oxide with concentrations of distilled water (φ =3, 1, 0.1 % by volume) in counterflow double-pipe heat exchanger.

2. Analysis of Heat Exchangers

The thermodynamics first law needs that the transfer rate of heat from the hot fluid be identical to the transfer rate of heat to the cold one, that is [8, 9]:

$$Q_c = (\rho\ Cp)_c u_c A_{cc} \times (T_{co} - T_{ci}) \qquad (1)$$

$$Q_h = (\rho\ Cp)_h u_h A_{ch} \times (T_{ho} - T_{hi}) \qquad (2)$$

Where $u = \frac{\dot{V}}{Ac}$ is the velocity of fluid and $\dot{V}$ is the volume flow rate of the fluid. The cross sectional area of the tube is given $A_c = \frac{\pi}{4}\ (d_i)^2$, $\dot{m} = \dot{V}\rho,\ and\ Ti,\ T_o$ are outlet and inlet temperature of the fluid at the test section, respectively. The rate of heat capacity for hot and cold fluid streams is given by:

$$C_h = \dot{m}_h Cp_h \quad and$$

$$C_c = \dot{m}_c Cp_c \qquad (3)$$

The rate of heat capacity of fluid is:

$Q = C_c(T_{co} - T_{ci})$ and

$$Q = C_h(T_{hi} - T_{ho}) \qquad (4)$$

The following form was used to express the transfer rate of heat in a heat exchanger:

$$Q = UA\ \Delta T_{lm} \qquad (5)$$

Where (ΔT_{lm}) is the logarithmic variance of mean temperature among hot and cold fluids (temperatures of outlet and inlet), (A) is the area of the heat transfer, and (U) is the overall coefficient of heat transfer.

To estimate the true temperature mean difference (ΔT_{lm}) between the two fluids, the following relation may be used to estimate the logarithmic variance of mean temperature according to the counter flow directions [9]:

$$Q = UA\ \frac{\Delta T_2 - \Delta T_1}{ln\ ln\ \left(\frac{\Delta T_2}{\Delta T_1}\right)} \qquad (6)$$

and

$$\Delta T_{lm} = \frac{\Delta T_2 - \Delta T_1}{ln ln\left(\frac{\Delta T_2}{\Delta T_1}\right)} = \frac{\Delta T_1 - \Delta T_2}{ln ln\left(\frac{\Delta T_1}{\Delta T_2}\right)} \qquad (7)$$

Where for counter flow:

$$\Delta T_1 = T_{hi} - T_{co}$$

$$\Delta T_2 = T_{ho} - T_{ci}$$

The area of the inner and outer surface is given by, [9].

$$A_{is} = d_i L \qquad (8)$$

and

$$A_{os} = \pi d_o L$$

and the thermal resistance of the tube wall in this case is:

$$R_{wall} = \frac{ln\left(\frac{r_o}{r_i}\right)}{2\pi k_t L} \qquad (9)$$

Where (k_t) is the thermal conductivity of the tube's wall material and (L) is the length of the tube. The total thermal resistance is given by:

$$\Sigma R = R_{total} = R_i + R_{wall} + R_o = \frac{1}{h_i A_{is}} + \frac{ln\left(\frac{r_o}{r_i}\right)}{2\pi k_t L} + \frac{1}{h_o A_{os}} \qquad (10)$$

$$Q = \frac{\Delta T_{lm}}{R} = UA\Delta T_{lm} = U_i A_{is}\Delta T_{lm} = U_o A_{os}\Delta T_{lm} \qquad (11)$$

Where $\left(\frac{W}{m^2{}^\circ C}\right)$ is identical to the unit of the ordinary convection coefficient (h). Omitting (ΔT_{lm}), equation (11) reduces to:

$$\frac{1}{UA} = \frac{1}{U_i A_{is}} = \frac{1}{U_o A_{os}} = \Sigma R = \frac{1}{h_i A_{is}} + R_{wall} + \frac{1}{h_o A_{os}} \qquad (12)$$

Substitute equation (9) in equation (12) gives:

$$U_o = \frac{1}{\frac{A_{os}}{h_i A_{is}} + \frac{A_{os}\, ln\left(\frac{d_o}{d_i}\right)}{2\pi k_t L} + \frac{1}{h_o}} \qquad (13)$$

or

$$U_o = \frac{1}{\frac{d_o}{h_i d_i} + \frac{d_o\, ln\left(\frac{d_o}{d_i}\right)}{2k_t} + \frac{1}{h_o}}$$

shell, given by

$$D_e = \frac{d_i^2 - d_o^2}{d_o} \qquad (17)$$

and Prandtl number is

$$Pr = \frac{\mu\, Cp}{k} \qquad (18)$$

After determining the value of (h_o), it can be inserted in eq. (14). Therefore, the only unidentified value would be (hi), which is estimated consequently. The value of the Nusselt number (Nu) can be calculated as follows:

$$Nu = \frac{h_i d_i}{k} \qquad (19)$$

The Reynolds number established by the equivalent shell diameter is:

$$Re = \frac{\rho u D_e}{\mu} \qquad (20)$$

2.1.The Improvement in Heat Transfer

The improvement in heat transfer using various occupied fluids is estimated by the following equation:

$$Enano = \frac{Nu_{av,nano} - Nu_{av,water}}{Nu_{av,water}} \qquad (21)$$

2.2.Calculations of Friction Factor and Pressure Drop

For the copper pipe turbulent flow, the factor of friction is estimated from Blasius correlation [10]:

$$f = 0.316Re^{-0.25} \tag{22}$$

Which is effective for Re$\leq 10^5$.

After equation (22) was substituted in the formula of Darcy, the pressure drop will be [11]:

$$\Delta p = f\left(\frac{L}{D}\right)(\rho u^2/2) \tag{23}$$

Where D is the inner tube inner diameter, L is the test section length, and Δp is the inner tube pressure drop.

3. Investigational Apparatus

Two kinds of operational fluid are tested (distilled water and metal oxide of Al_2O_3 as Nanofluid with distilled water at φ = 3, 1, 0.1 % concentrations by volume.

3.1.Test Rig and Investigational Apparatus

The rig composed of the test section (double pipe heat exchanger), the hot fluid internal cycle is consisting of hot fluid tank (3 litters), pump, heater, digital temperature reader, six thermocouples (K–type), the control board, flow meter, pump, water tanks (20 litters) and (500 litters) for supplying cold water, flow meter, piping system and control valves as shown in Figure 1. Most of these parts are manufactured, and care was given to the connected section through re-fixing and operation to avoid any kind of fluid leakage. To avoid dissipation of heat, the hot cycle was insulated using Good multi-layer insulator.

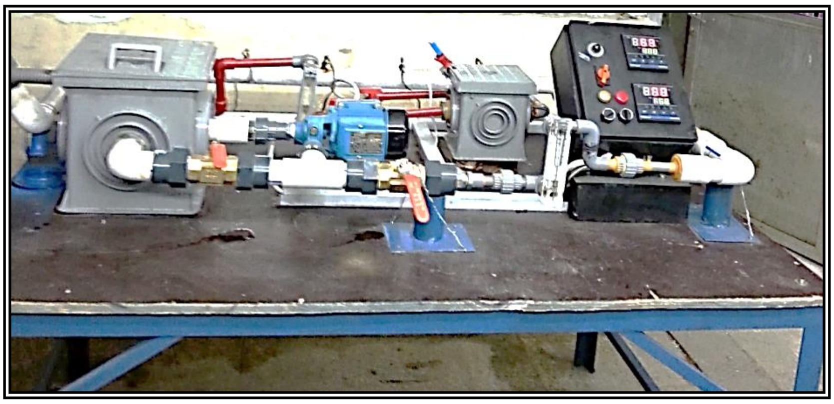

Figure 1: Experimental test rig.

3.2.The Test Section

The test segment was a heat exchanger with double pipes, and it made of concentric pipes. PVC tube was selected as the outside pipe of the test section, and the Copper tube was chosen as an inner tube. The warm fluid moves through the internal tube, whereas the freezing fluid moves through the annulus.

3.3.The Control Board

The control board comprises controls to open and close the circulating pumps, the electrical circuit to control the hot fluid inlet temperature through the switch, electrical heater, and controller and display screen with the setting, selector switch and digital reader with the display screen to read the temperature of the thermocouples.

3.4.Measuring Devices

3.4.1. Thermocouples

Six thermocouples (K–type) are utilized to measure the temperatures in various locations along with the test rig. Four thermocouples are used to measure the temperatures along the surface of the inner pipe at the heated test section. Two thermocouples are immersed in the fluid to measure the inlet temperatures of the hot and cold fluids inlet to the test section. All thermocouples are linked to the control board.

3.4.2. Digital Thermometer

A digital temperature reader is used to measure the mean temperature of the cooling water outlet and ambient temperature.

4. Results and Discussion

In this work, heat transfer and pressure drop for the specified double pipe heat exchanger were calculated experimentally. Nusselt number and friction factor are utilized to identify the heat transfer and pressure drop, respectively for the working fluids (distilled water and metal oxide of Al_2O_3 as nanofluid with distilled water at φ = 3, 1, 0.1 % concentrations by volume. Experimental outcomes of heat transfer and pressure drop are compared with other results. All the investigations are carried out for inlet fluid temperatures (T_{in}=40, 50, 60 and 70 ^{o}C).

4.1.Inlet Temperature Effect

The recorded data from the experiments for the inner pipe local temperature using water with diverse values of flow rate and inlet temperature are illustrated in Figures 1 to 3. For high values of inlet temperature, it was detected a high temperature variance. For (70 °C) inlet temperature, (30-34) Temperature variance was detected. Whereas for (40 °C) inlet temperature, (8-10) Temperature variance was recorded. The reason for that goes to the volume flow rate increasing effect and the high heat transfer among the two fluids.

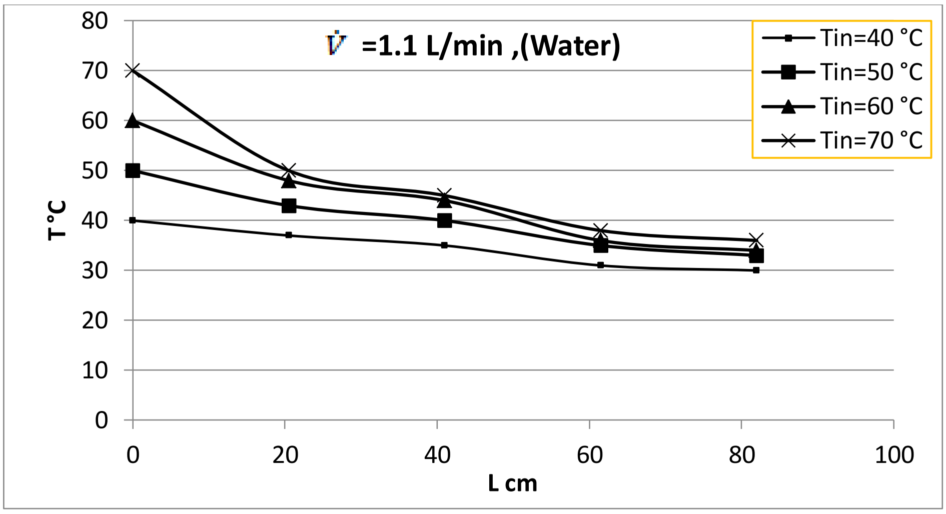

Figure 2: Temperature along the inner pipe for water at the flow rate (1.1 L/min).

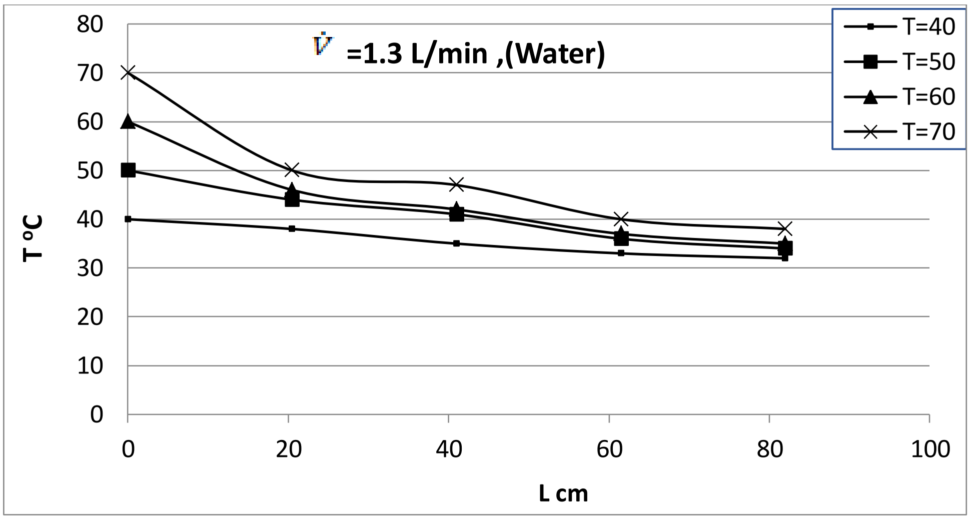

Figure 3: Temperature along the inner pipe for water at the flow rate (1.3 L/min).

Figures 4 to 6 present similar outcomes but for using nanofluid (AL_2O_3 and distilled water) with a concentration of 0.1% which give temperature variance (15-28) for temperature inlet (70 °C) and (7-9) for temperature inlet of (40 °C).

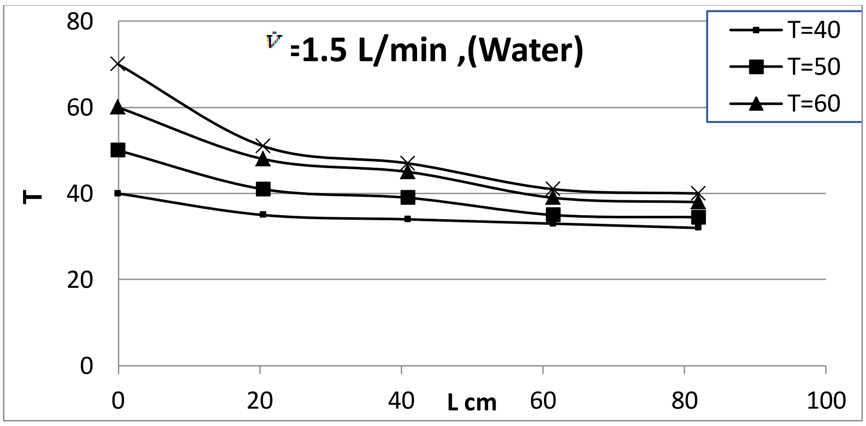

Figure 4: Temperature along the inner pipe for water at the flow rate (1.5 L/min).

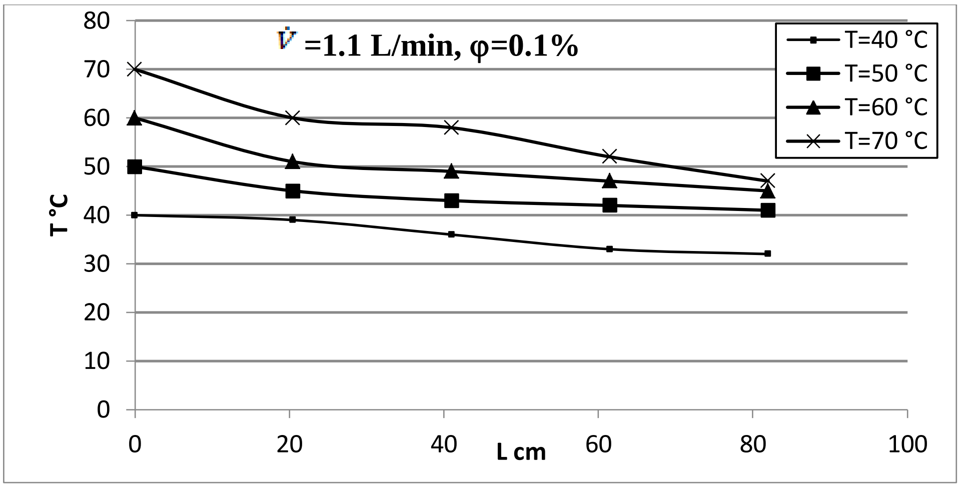

Figure 5: Temperature along the inner pipe for Al_2O_3 nanofluid at a flow rate (1.1 L/min) and ϕ=0.1%.

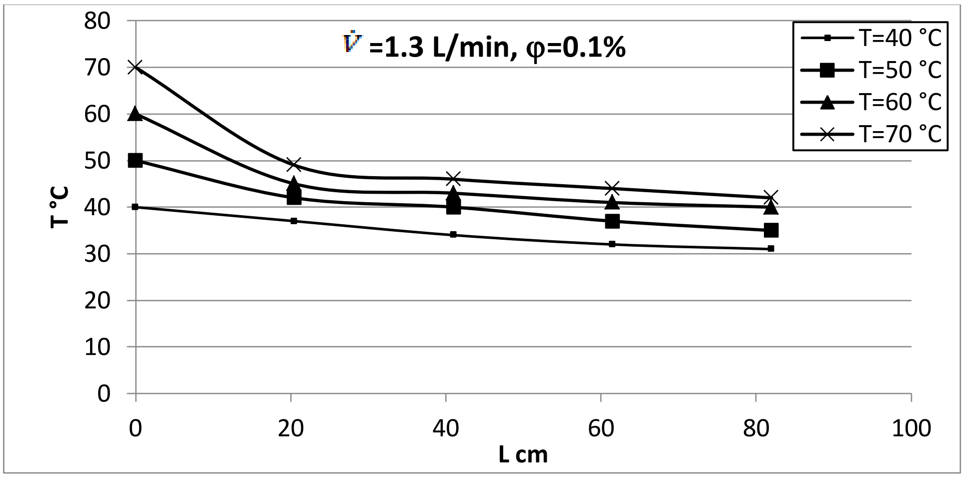

Figure 6: Temperature along the inner pipe for Al_2O_3 nanofluid at a flow rate (1.3 L/min) and ϕ=0.1 %.

Figures 7 to 9 present the equal relation for 1% concentration nanofluid which gives (12-14) temperature variance for (70 °C) inlet temperature while it gives (6-8) temperature variance for (40 °C) inlet temperature.

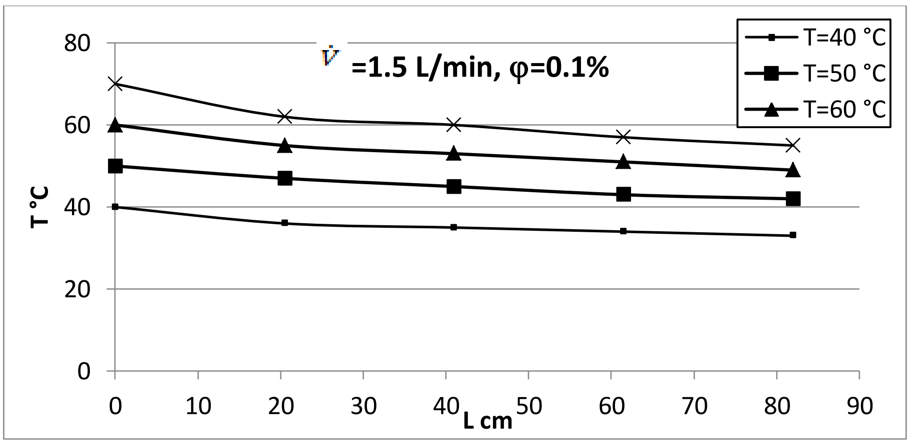

Figure 7: Temperature along the inner pipe for Al_2O_3 nanofluid at a flow rate (1.5 L/min) and ϕ=0.1%.

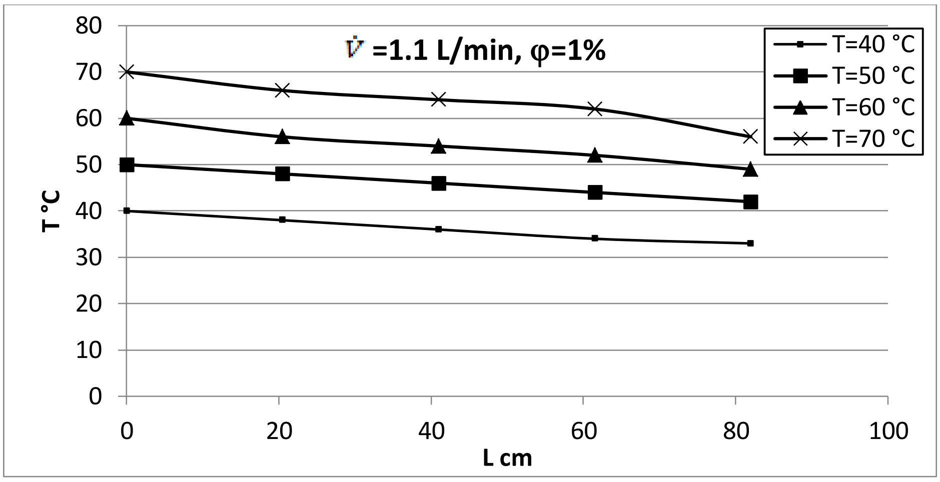

Figure 8: Temperature along the inner pipe for Al_2O_3nanofluidat flow rate (1.1 L/min) and ϕ=1%.

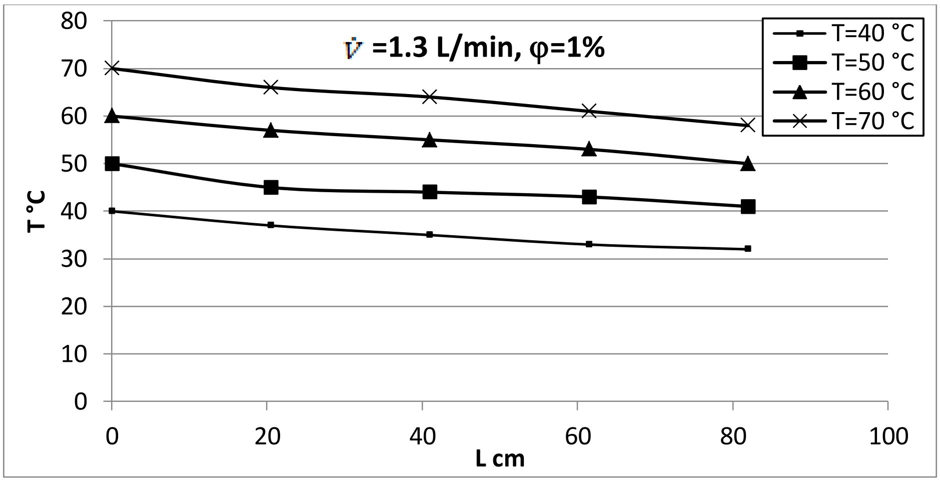

Figure 9: Temperature along the inner pipe for Al_2O_3 nanofluid at a flow rate (1.3 L/min) and ϕ=1 %.

Figures 10 to 12 present the same relation for Nanofluid with (3%) concentration, which gives (12-14) temperature variance, higher variance, for (70 °C) inlet temperature whereas it gives (6-7) temperature variance for (40 °C) inlet temperature. The temperature alteration dissimilarity caused by the variation of Nanofluid physical features depends on the concentration such as rising Brownian motion and thermal conductivity of Nanoparticle causing by that a rise in the fluid heat extraction. The Nusselt number values rise with rising of inlet temperature and Reynolds number as illustrated in Figures 13 to 16 for all fluids. The rise in the rate of flow preserves a large incline in the temperature near to the wall of the tube and in turn, raises the improvement in the transfer of heat. In addition, the alteration in fluid features raises the Nusselt number values as illustrated in the same figures. For Nanofluid, the Nusselt number rise with rising concentration (ϕ=0.1, 1and 3%). The nanoparticles Brownian motion was used to clarify that, As the concentration rises, the Nusselt number rises due to the nanoparticles volume fraction increasing, which cause an increase in the Nanofluid effective thermal conductivity. The resistance of the thermal diffusion of the boundary layer in the laminar sublayer decreases by the thermal conductivity improvement, due to the liquid molecular – level layering at liquid/particle interface (wet ability).

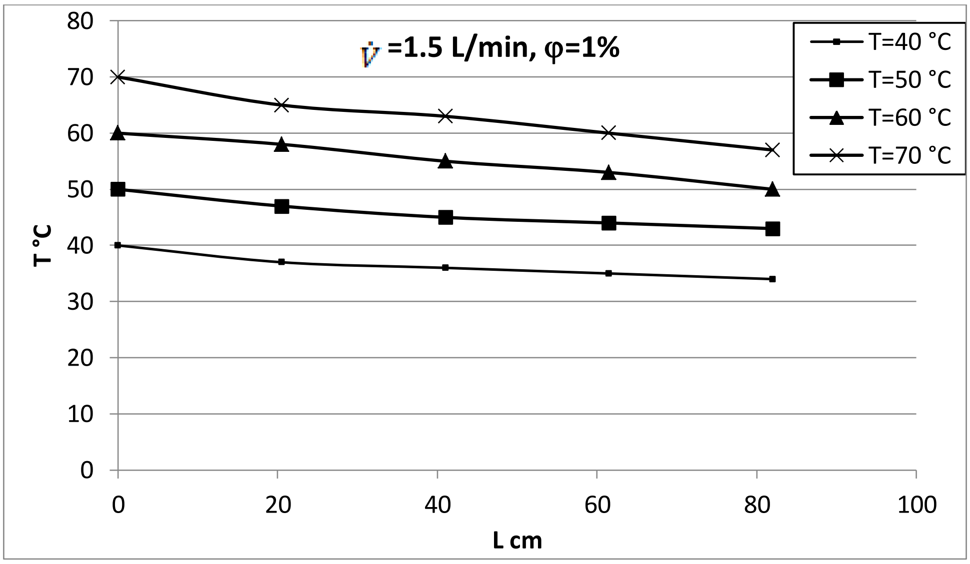

Figure 10: Temperature along the inner pipe for Al_2O_3 nanofluid at a flow rate (1.5 L/min) and ϕ=1%.

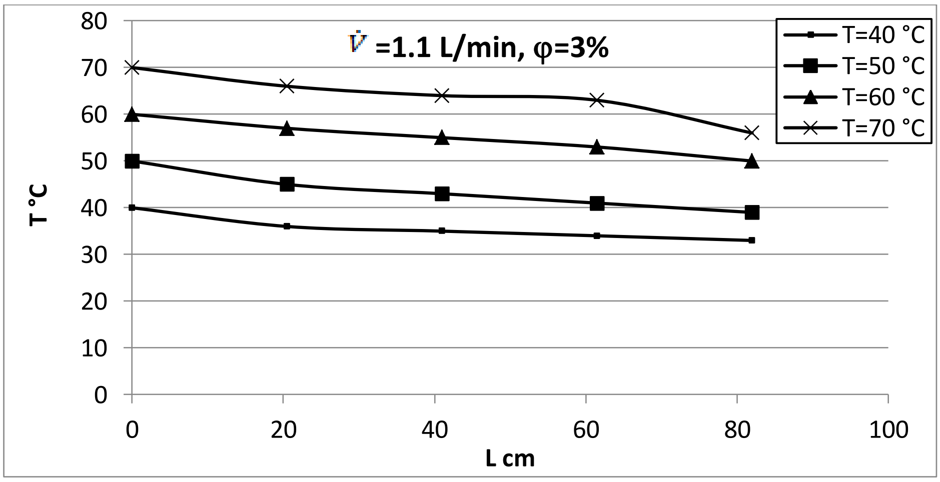

Figure 11: Temperature along the inner pipe for Al_2O_3 nanofluid at a flow rate (1.1 L/min) and ϕ=3%.

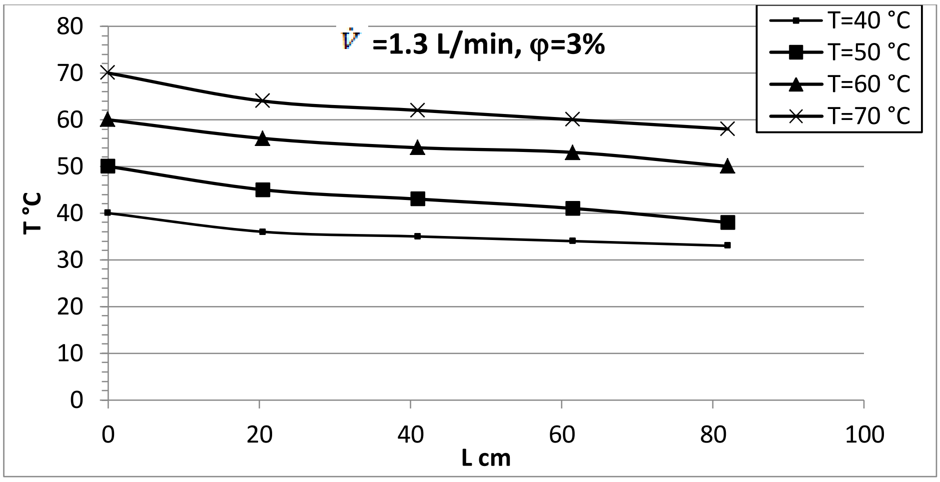

Figure 12: Temperature along the inner pipe for Al_2O_3 nanofluid at a flow rate (1.3 L/min) and ϕ=3%.

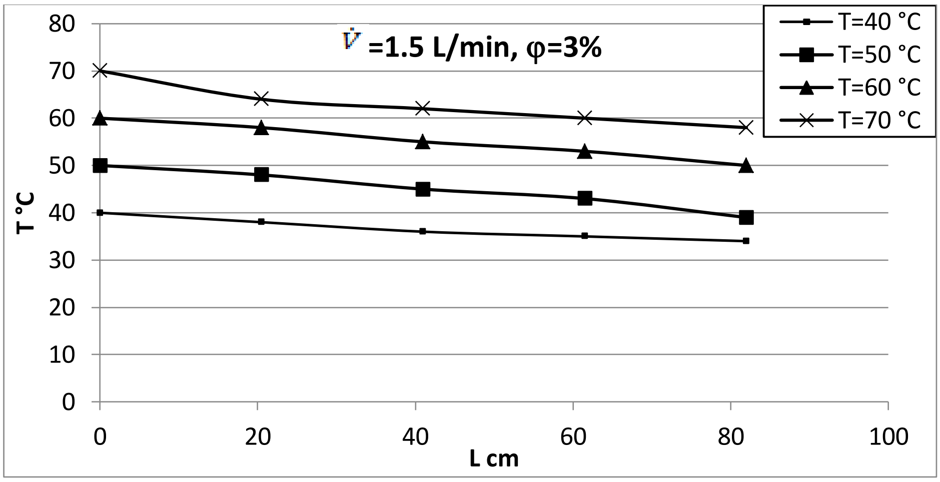

Figure 13: Temperature along the inner pipe for Al_2O_3 nanofluid at a flow rate (1.5 L/min) and ϕ=3%.

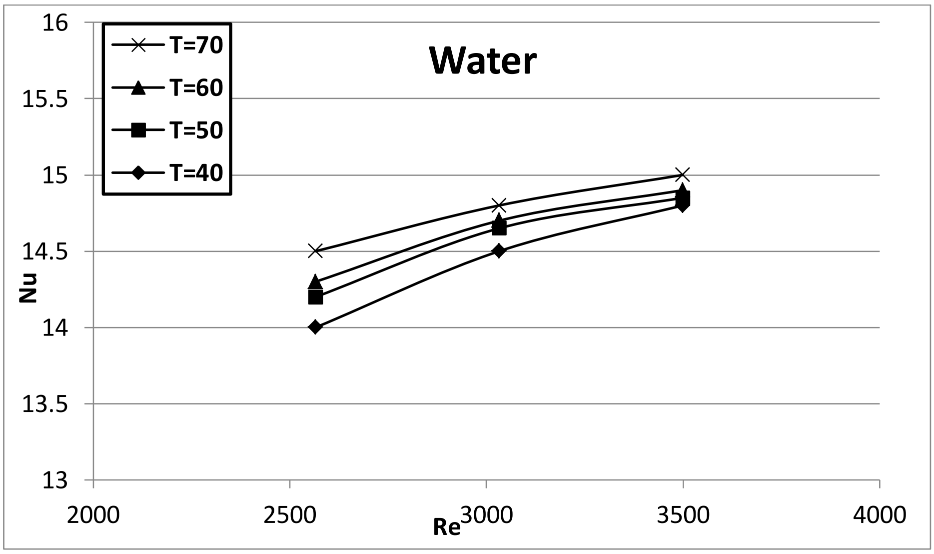

Figure 14: Nusselt number for water at Tin =40, 50, 60 and 70 oC.

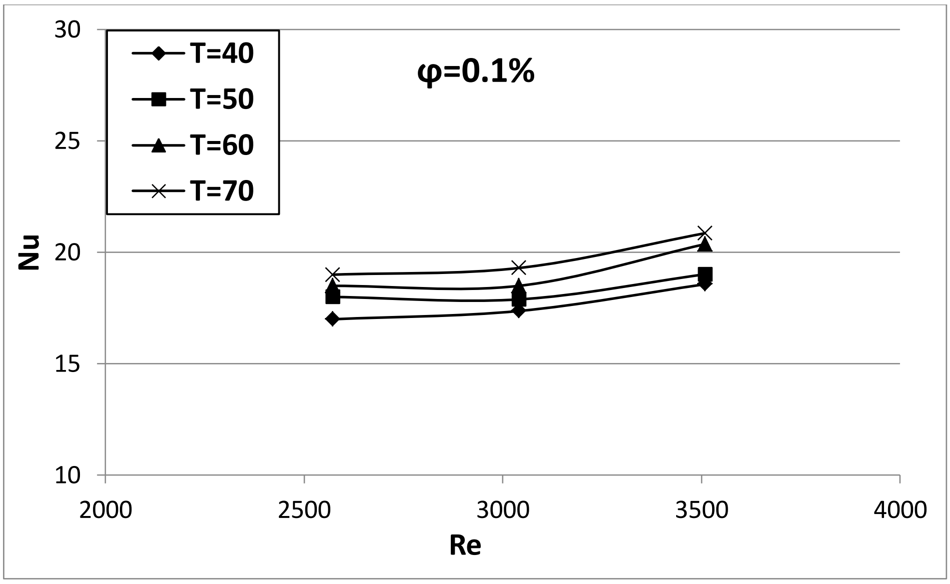

Figure 15: Nusselt number for Al_2O_3 nanofluid at ϕ=0.1% at Tin =40, 50, 60 and 70oC.

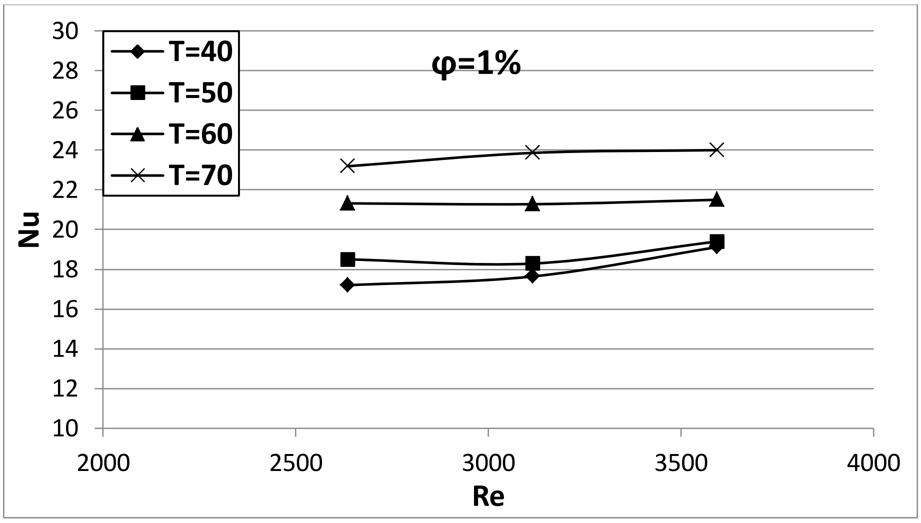

Figure 16: Nusselt number for Al_2O_3 nanofluid ϕ=1 % at Tin =40, 50, 60 and 70 oC.

The average values of Nusselt number at the four inlet temperature and at fixed Reynolds number is estimated and presented in Figure 17. The correlations amid Reynolds number and Nusselt number was utilized by using each of the working fluids power method as shown below.

1. For water: $Nu = 4.68\ Re^{0.1419}$ $(2566 \leq Re \leq 3500)$ (24)
2. For Al_2O_3 nanofluid at ϕ=0.1%:

$Nu = 2.27\ Re^{0.2631}$ $(2573 \leq Re \leq 3509)$ (25)

3. For Al_2O_3 nanofluid at ϕ=1%:

$Nu = 6.26\ Re^{0.1472}$ $(2636 \leq Re \leq 3595)$ (26)

4. For Al_2O_3 nanofluid at ϕ=3%:

$Nu = 2.37\ Re^{0.28}$ $(2774 \leq Re \leq 3783)$ (27)

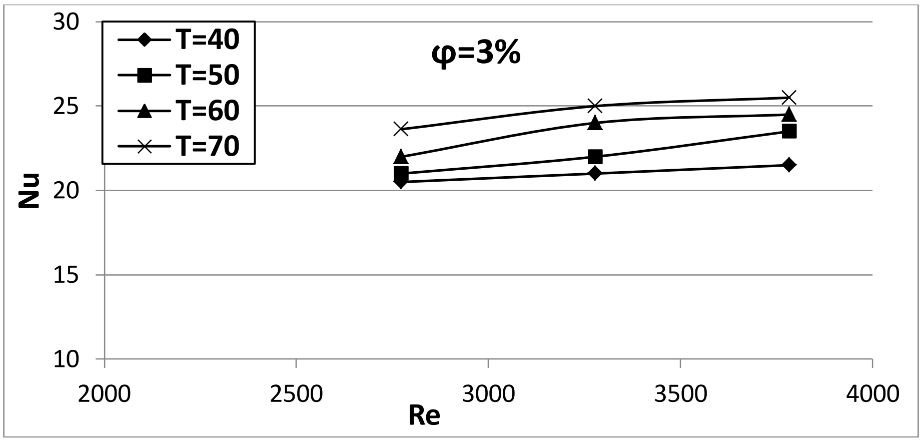

Figure 17: Nusselt number for Al2O3 nanofluid ϕ=3 % at Tin =40, 50, 60 and 70 oC.

4.2. HYDRODYNAMIC CHARACTERISTICS OF THE FLOW

Friction factor can be estimated by using the following correlation [10]:

$$f = 0.316Re^{-0.25} \tag{28}$$

and the pressure drop from the expression [11]:

$$\Delta p = f\left(\frac{D}{L}\right)(\rho u^2/2) \tag{29}$$

Figures 18 to 21 display the difference of pressure drop with Reynolds number for water and Al_2O_3 as nanofluid at concentrations (ϕ=0.1, 1and 3%). The pressure drop rises as Reynolds number increases. Less pressure drop was (89.6 pa) for water at (1.1 L/min) flow rate. Also for nanofluid, the pressure drop rise with rising concentration (ϕ=0.1, 1 and 3%). As the concentration rises, the pressure drop rises due to the rise of fluid viscosity and density.

For friction factor, Figures 22 to 25 display the difference of friction factor with Reynolds number for water and Al_2O_3 as nanofluid at concentrations (ϕ=0.1, 1and 3%), the friction factor drops as Reynolds number rises. For nanofluid, the friction factor drop with rising concentration (ϕ=0.1, 1 and 3%) to (0.04029). This is due to drops of the velocity of the fluid. Figure 26 displays the difference of Nusselt number with Reynold number for Al_2O_3 at an inlet temperature of 70 °C for three standards of concentrations (φ= 0.1,1 and 3%). It displays that as Reynold number rises, the Nusselt number rises too for all cases. High Nusselt number was achieved with a concentration of 3%.

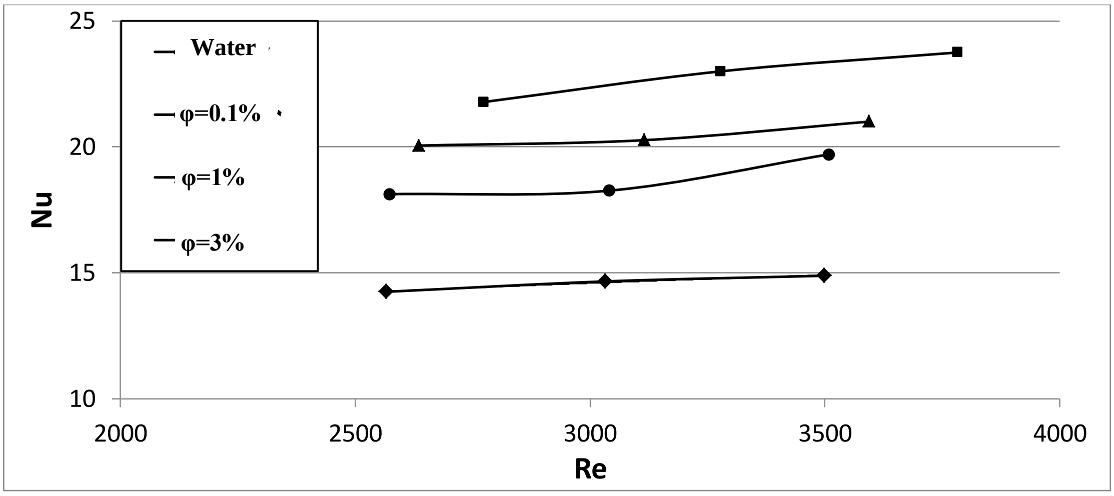

Figure 18: Average Nusselt number for water and Al_2O_3 nanofluid at ϕ=0.1, 1and 3%.

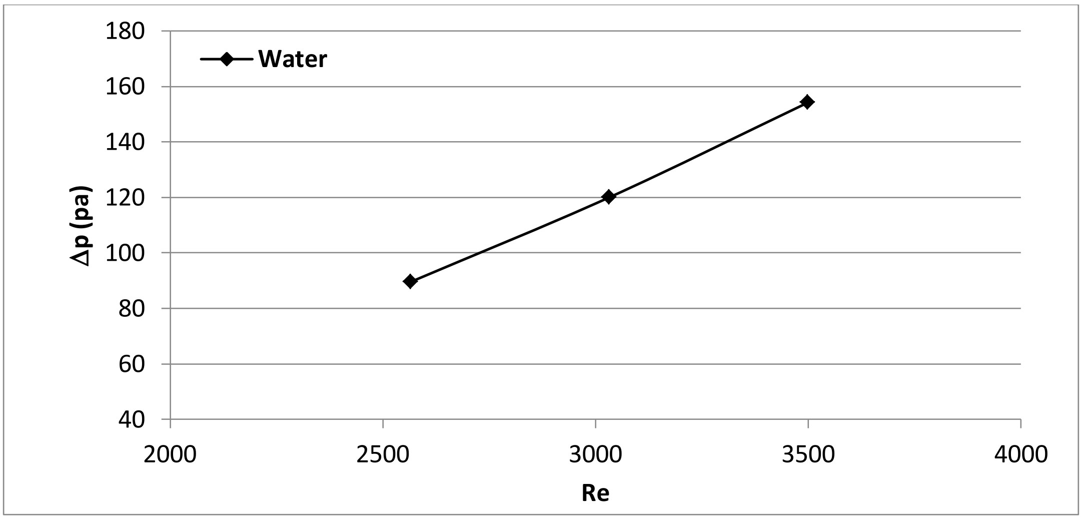

Figure 19: Pressure drop for water.

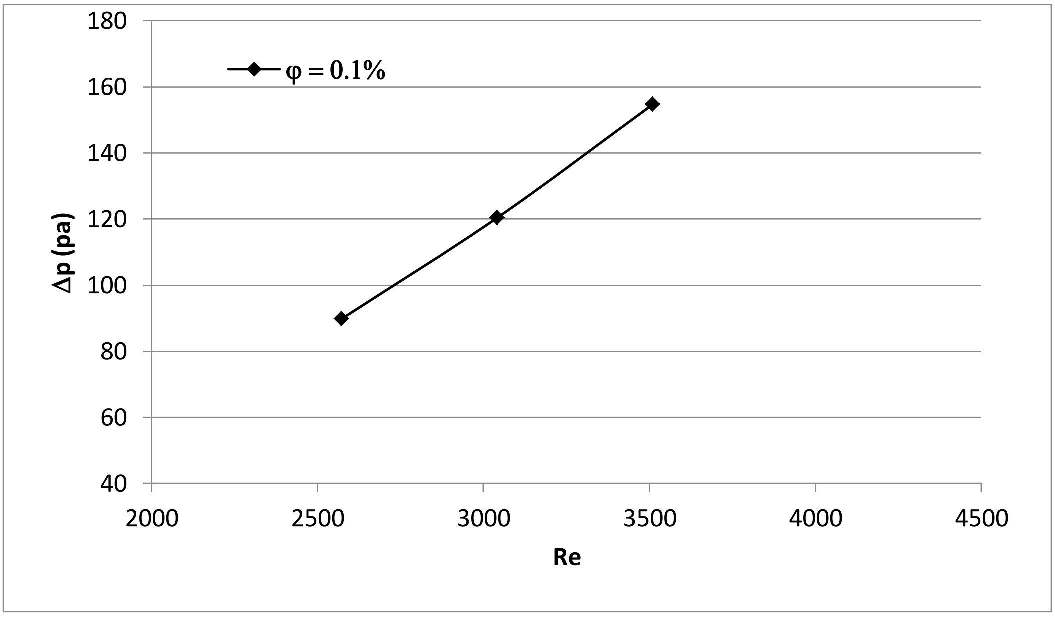

Figure 20: Pressure drop for Al_2O_3 nanofluid at ϕ=0.1%.

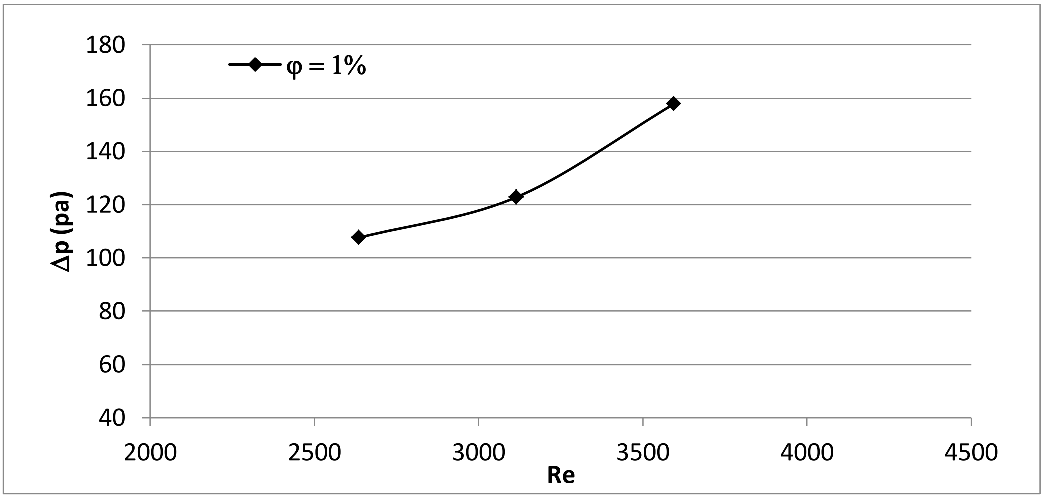

Figure 21: Pressure drop for Al_2O_3 nanofluid at ϕ=1%.

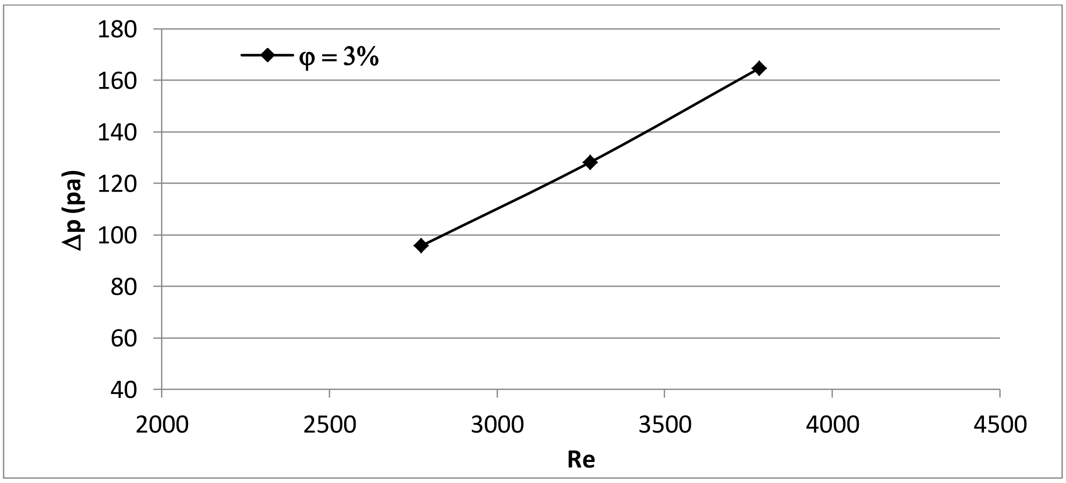

Figure 22: Pressure drop for Al_2O_3 nanofluid at ϕ=3 %.

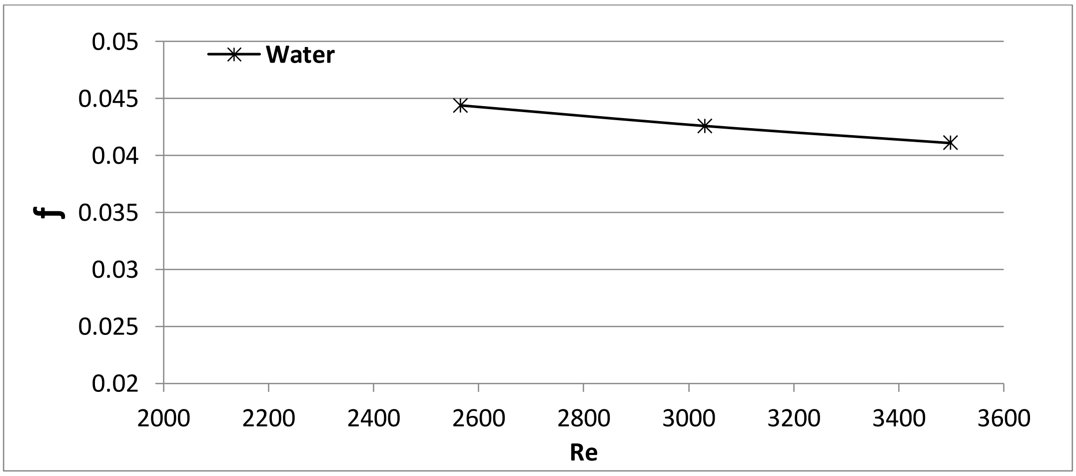

Figure 23: Friction factor for water.

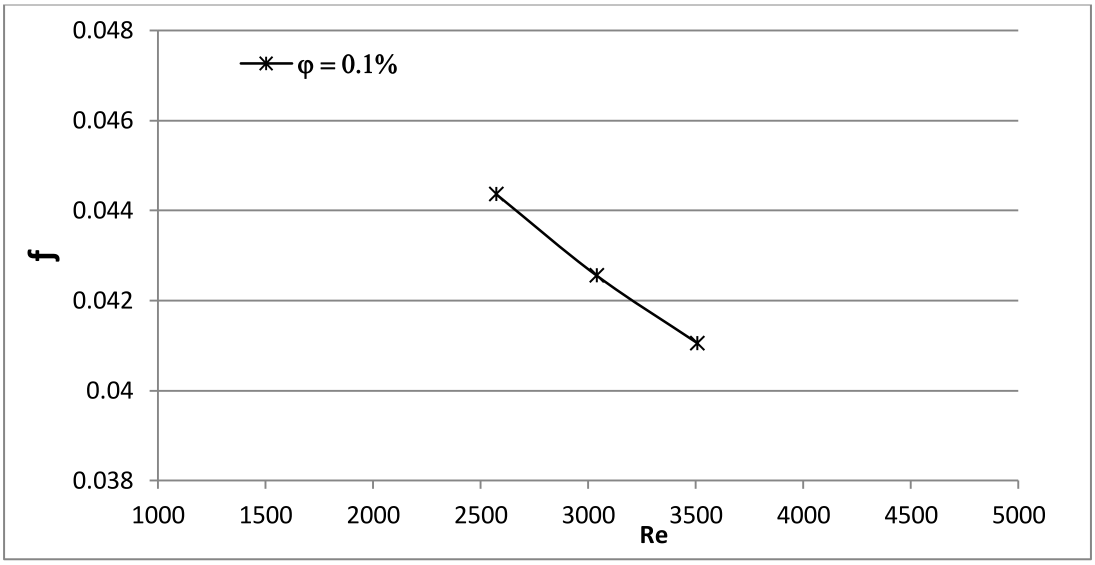

Figure 24: Friction factor for Al_2O_3 nanofluid at ϕ=0.1 %.

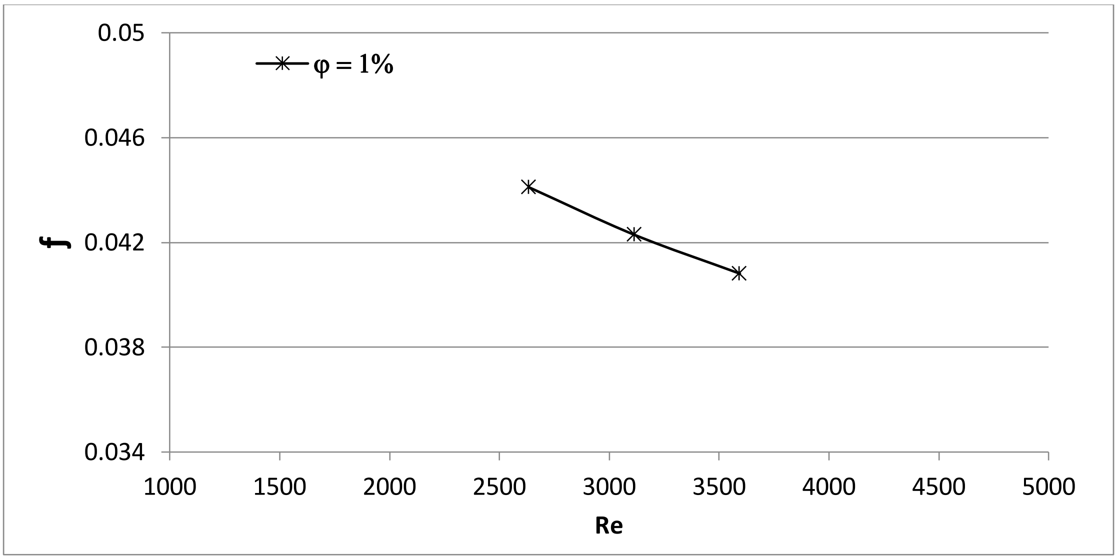

Figure 25: Friction factor for Al_2O_3 nanofluid at ϕ=1%.

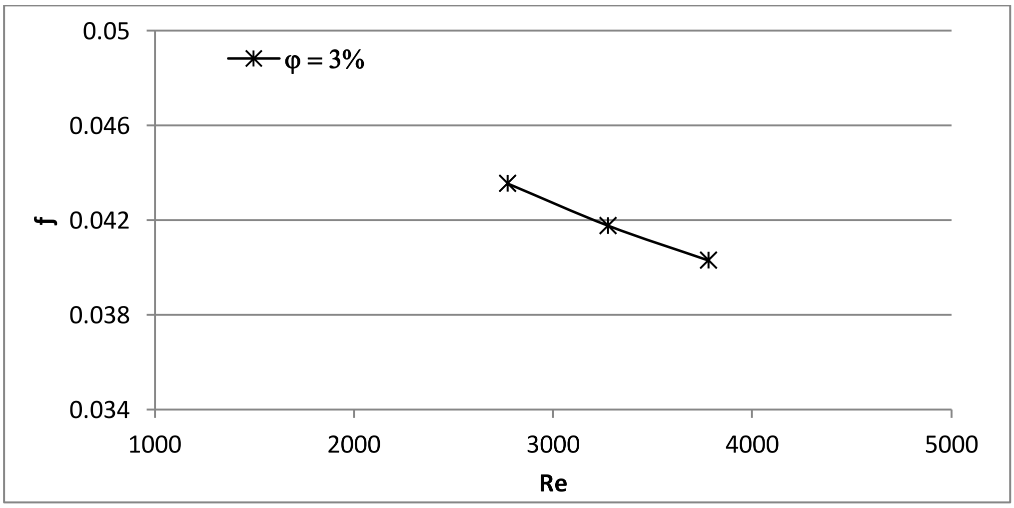

Figure 26: Friction factor for Al_2O_3 nanofluid at ϕ=3%.

Figure 27 displays the difference of Nusselt number with Reynold number for two fluids: distilled water and Nanofluid (AL_2O_3+distilled water) with concentration 3%, which is better than the distilled water. This could be connected to the large thermal conductivity of the solid particles (AL_2O_3). Hence, using 3%, AL_2O_3 Nanofluid will improve the transfer of heat and increases the heat exchanger efficiency.

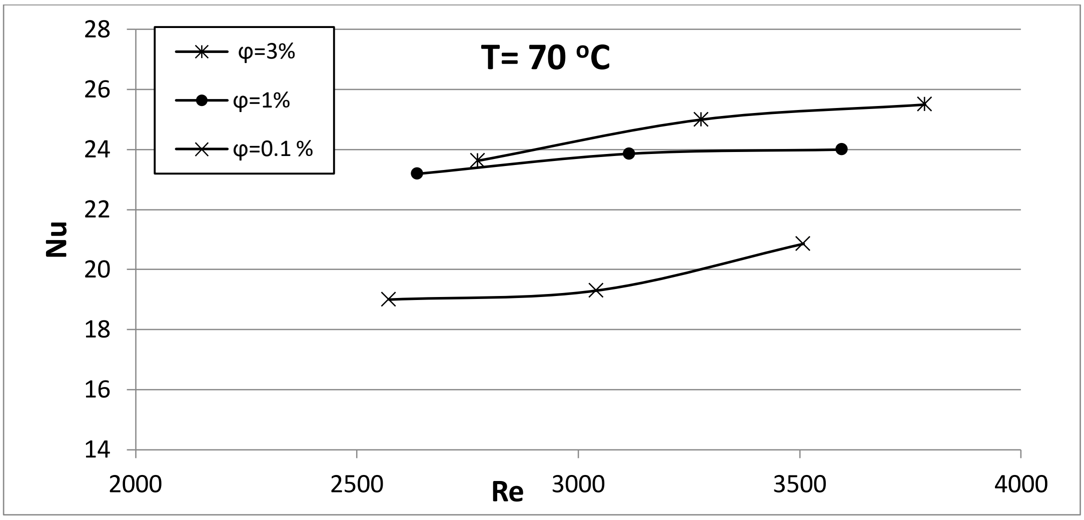

Figure 27: Nusselt number for Al_2O_3 with different concentrations for inlet Temperature 70 °C.

4.3. Results and Discussion

Figure 28 shows a comparison between the theoretical and investigational Nusselt number when using water in the heat exchanger. It displays that the investigational Nusselt number is flatter than the theoretical one. This could be connected to the losses related to the investigational part, which are not taken into account theoretically. However, both outcomes show a rise in Nusselt number with water temperature. Figure 29 and 30 indicate comparison for Nusselt number correlation of the present experimental results with the published work [12] and [4], respectively, and the comparison displays a good agreement.

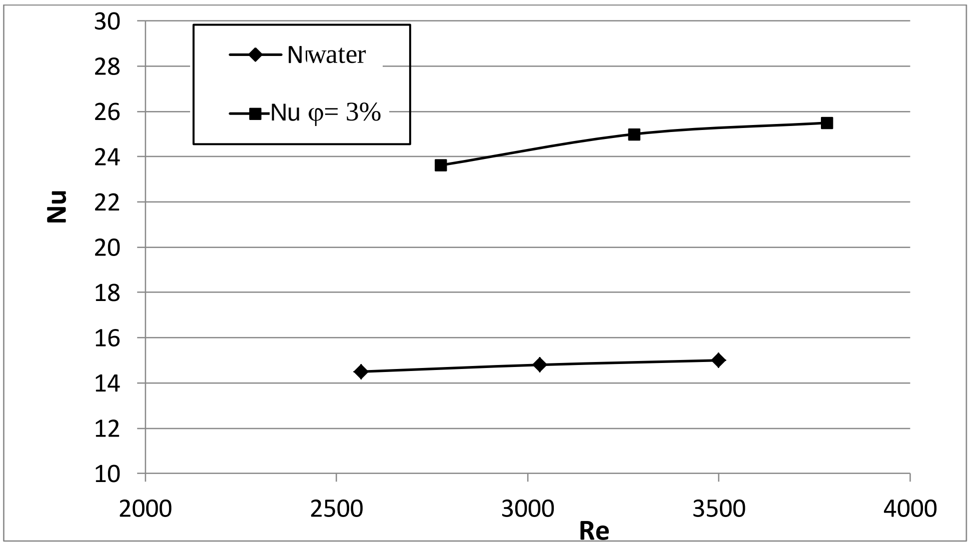

Figure 28: Nusselt number for water and Al_2O_3 with ϕ= 3% for inlet temperature 70°C.

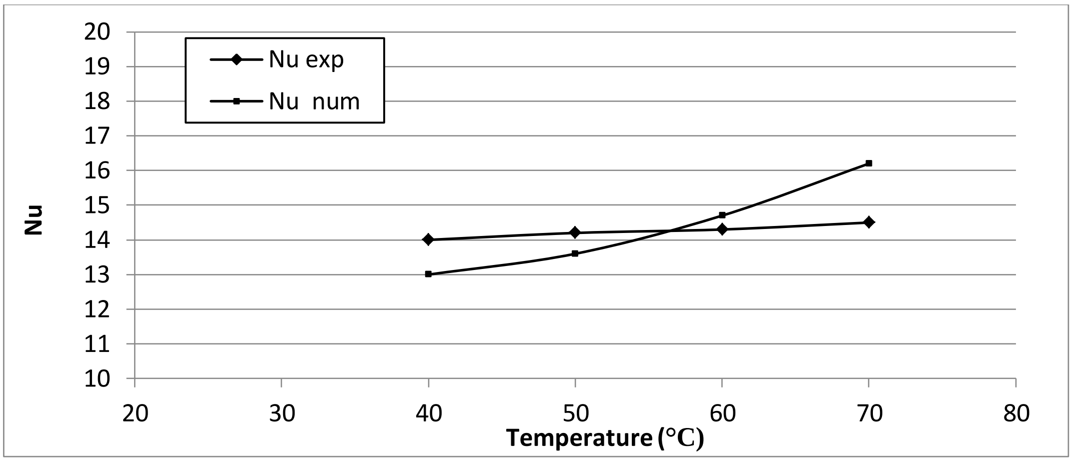

Figure 29: Comparison between the experimental and numerical of the present results for water.

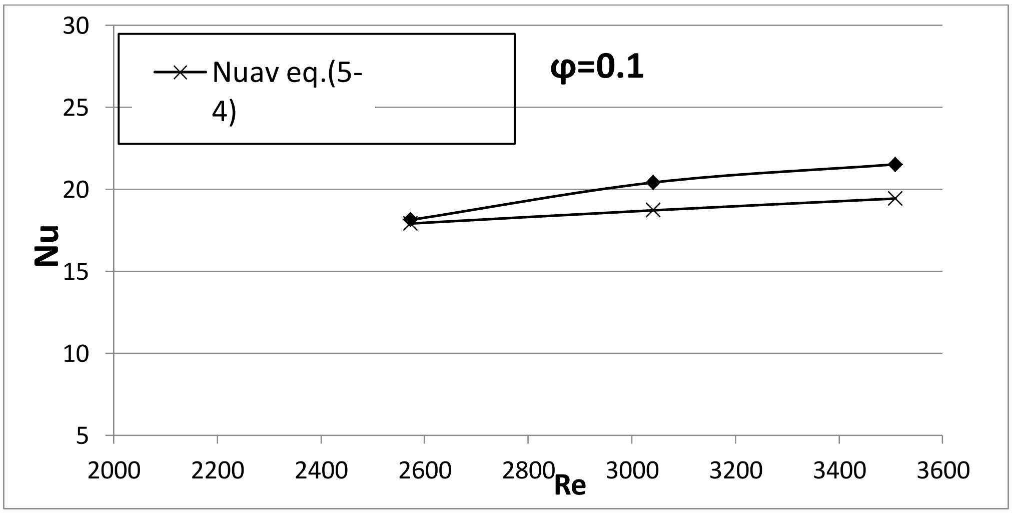

Figure 30: Comparison of present results with Vajjha RS work [12].

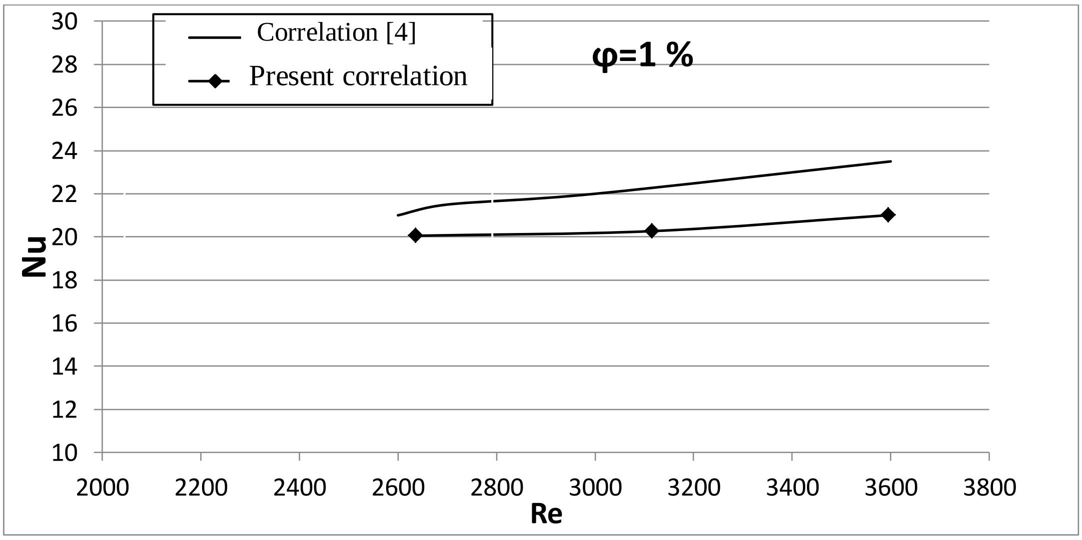

Figure 31: Comparison of present results with Heyhat M. M. work [4].

5. CONCLUSIONS

The following facts can be determined from the present work:

1. The temperature of the inner tube rises as stirring from the water to nanofluid (φ=3%) whereas the average temperature alongside the inner pipe, in general, stay constant with the rise in flow rate.
2. The alteration in fluid features raises the values of Nusselt number.
3. The Nusselt number rise with rising concentration (φ=0.1, 1and 3%), as the concentration increases the Nusselt number increases.
4. The maximum improvement was (40.2%) recognized for nanofluid with concentration (φ=3%) at flowing in temperature (70 ^oC), and the smallest improvement was (18.2 %) recognized for Al_2O_3 as nanofluid at φ=0.1% and inlet temperature (40 ^oC).
5. The pressure drop rises with growing concentration and friction factor drop as Reynolds number rises. For nanofluid, the friction factor drops with growing concentration (φ=0.1, 1and 3%) to (0.04029).
6. The best operational fluid for everyday technology is the Al_2O_3 which gives (0.402) improvement, (164.78 pa) pressure drop and (0.04029) friction factor for (φ= 3%).

Acknowledgements

Authors would like to thank University of Technology/Mechanical Engineering Department, Training and Workshop Center and University of Almustansiriya/Mechanical Engineering Department for their support.

References

[1] Cheng, L., 2009. Nanofluid heat transfer technologies. *Recent Patents on Engineering*, *3*(1), pp.1-7.

[2] Mansour, R.B., Galanis, N. and Nguyen, C.T., 2011. Experimental study of mixed convection with water–Al2O3 nanofluid in inclined tube with uniform wall heat flux. *International Journal of Thermal Sciences*, *50*(3), pp.403-410.

[3] Murugesan, C., Tamilkolundu, S., "Mechanism of Forced Convective Heat Transfer in Al_2O_3/Water Nanofluid under Laminar and Turbulent Flow", 2nd International Conference on Chemical, Ecology and Environmental Sciences (ICCEES'2012) Singapore April 28-29, pp 71-75.

[4] Heyhat, M.M., Kowsary, F., Rashidi, A.M., Esfehani, S.A.V. and Amrollahi, A., 2012. Experimental investigation of turbulent flow and convective heat transfer characteristics of alumina water nanofluids in fully developed flow regime. *International Communications in Heat and Mass Transfer*, *39*(8), pp.1272-1278.

[5] Demir, H., Dalkilic, A.S., Kürekci, N.A., Duangthongsuk, W. and Wongwises, S., 2011. Numerical investigation on the single phase forced convection heat transfer characteristics of TiO2 nanofluids in a double-tube counter flow heat exchanger. *International Communications in Heat and Mass Transfer*, *38*(2), pp.218-228.

[6] Akbari, M., Galanis, N. and Behzadmehr, A., 2011. Comparative analysis of single and two-phase models for CFD studies of nanofluid heat transfer. *International Journal of Thermal Sciences*, *50*(8), pp.1343-1354.

[7] Moraveji, M.K., Darabi, M., Haddad, S.M.H. and Davarnejad, R., 2011. Modeling of convective heat transfer of a nanofluid in the developing region of tube flow with computational fluid dynamics. *International communications in heat and mass transfer*, *38*(9), pp.1291-1295.

[8] Hasan, W.F., 2008. *Theoretical and Experimental Study to Finned Tubes Cross Flow Heat Exchanger*, MSc, thesis, University of Technology, Iraq-Baghdad.

[9] Incropera, F. B., and Doot, D. B., 1986. "Principles of Heat Transfer", McGraw-Hill Co.

[10] Munson, B.R., Okiishi, T.H., Huebsch, W.W. and Rothmayer, A.P., 2013. *Fluid mechanics*. Singapore: Wiley.

[11] American Society of Heating Refrigeration, and Air Conditioning Engineers, 2009. “ASHRAE Fundamentals Handbook “, Chapter 22, pp.22.1-22.21.

[12] Vajjha, R.S., Das, D.K. and Kulkarni, D.P., 2010. Development of new correlations for convective heat transfer and friction factor in turbulent regime for nanofluids. *International journal of heat and mass transfer*, *53*(21-22), pp.4607-4618.